UFSM

CIÊNCIA e NATURA

ISSN 2179-460X
OPEN ACCESS

Ci. e Nat., Santa Maria, v. 46, spe.3, e86798, 2024 • https://doi.org/10.5902/217946086798
Submitted: 23/02/2024 • Approved: 17/05/2024 • Published: 08/11/2024

II Feira de Ciências, Tecnologia e Inovação da UFSM-CS

Structural analysis and design of a self-supporting wooden bridge designed by Leonardo Da Vinci

Análise estrutural e dimensionamento de ponte autoportante em madeira criada por Leonardo Da Vinci

Lucas Alves Lamberti[I], Rafael Domingues Della Pace[I], Lucas Tavares Cardoso[I], Carla Fernanda Perius[I], Fábio Beck[I], Diogo Pauletti[I]

[I]Universidade Federal de Santa Maria, RS, Brazil

ABSTRACT

Leonardo Da Vinci created several bridges throughout his life, including a highly practical self-supporting bridge. This research aimed to investigate the geometry of the self-supporting bridge structure, the transmission of loads along the bars, and to conduct design simulations. Initially, calculations were developed for the length, height, and angles of the bridge. Subsequently, support reactions for each bar composing the bridge were calculated, followed by the design of the bridge, considering wood as the material used. Finally, simulations were conducted for bridge lengths of 4 m, 5 m, 6 m, and 7 m. It was found that for each situation, there are various possibilities for bridges, with variations in height and angles of the bridge as well as different bar sizes. The results showed that taller bridges may be more efficient; however, this would complicate practical crossings. Therefore, it is necessary to limit the height, and the optimal point found in this research was a bridge height-to-length ratio of 0.30. Nevertheless, it is still possible to adapt the bridge access to smooth the passage, requiring further in-depth studies.

Keywords: Bridge; Support reaction; Structure; Load

RESUMO

Leonardo Da Vinci criou algumas pontes ao longo de sua vida, entre elas uma ponte autoportante bastante prática. Esta pesquisa buscou investigar a geometria da estrutura da ponte autoportante, a transmissão de cargas ao longo das barras e realizar simulações de dimensionamento. Primeiramente, foram desenvolvidos cálculos do comprimento, altura e ângulos da ponte. Em seguida, foram desenvolvidos cálculos das reações de apoio de cada barra que compõe a ponte, para, então, realizar o dimensionamento da ponte considerando madeira como material utilizado. Por último, foram

simuladas situações de 4 m, 5 m, 6 m e 7 m de comprimento da ponte. Foi constatado que para cada situação existem diversas possibilidades de pontes, com variações de altura e ângulos da ponte, além de diferentes tamanhos de barras. Os resultados mostraram que pontes mais altas podem ser mais eficientes, no entanto, isso dificultaria a travessia em situação prática. Portanto, é preciso limitar a altura e o ponto ótimo encontrado nesta pesquisa foi de uma relação altura e comprimento da ponte de 0,30. No entanto, ainda é possível adaptar o acesso à ponte para suavizar a passagem, o que exige estudos mais aprofundados.

Palavras-chave: Ponte; Reação de apoio; Estrutura; Carregamento

1 INTRODUCTION

1.1 The Da Vinci's self-supporting bridge

Leonardo Da Vinci designed several innovative bridges for his time, with most of them dating back to the early years after his arrival to Milan in 1482. The self-supporting bridge is one of the most ingenious bridges due to its construction and structural simplicity (Figure 1). It is, indeed, a structure composed of simple beams with a circular cross-section (in the original design), intended to be assembled without the need for fastenings or joints. Once assembled, the weight of the bridge exerts pressure between the bars, preventing the structure from collapsing. More pressure at the top of the bridge produces greater stability (Hipátia Engenharia, 2022; Lima, et al., 2017).

Figure 1 – Da Vinci's drawing the self-supporting bridge

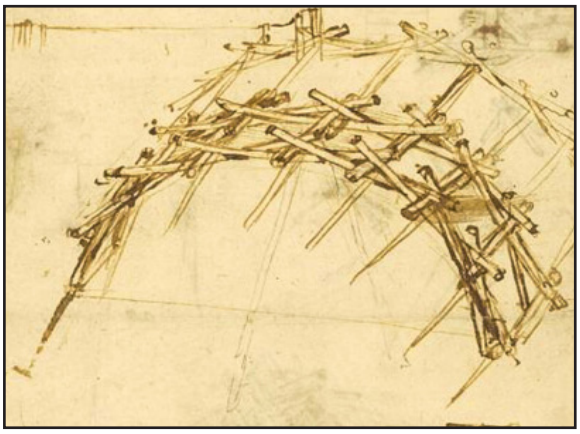

Source: Engenho e arte (2020)

The project envisioned the swift and unpredictable passage of soldiers over a river, contributing to the element of surprise, crucial for the success of a battle (Morumbi Sul, 2021; Scantamburlo, 2017). The primary purpose, in fact, was military, as Leonardo developed the project for Cesare Borgia, with whom he worked as a military engineer (Engenho E Arte, 2020).

1.2 Structure

The assembly is performed sequentially from one end to another (Figure 2), interleaving the longitudinal and cross-bars.

Figure 2 – Assembling the self-supporting bridge

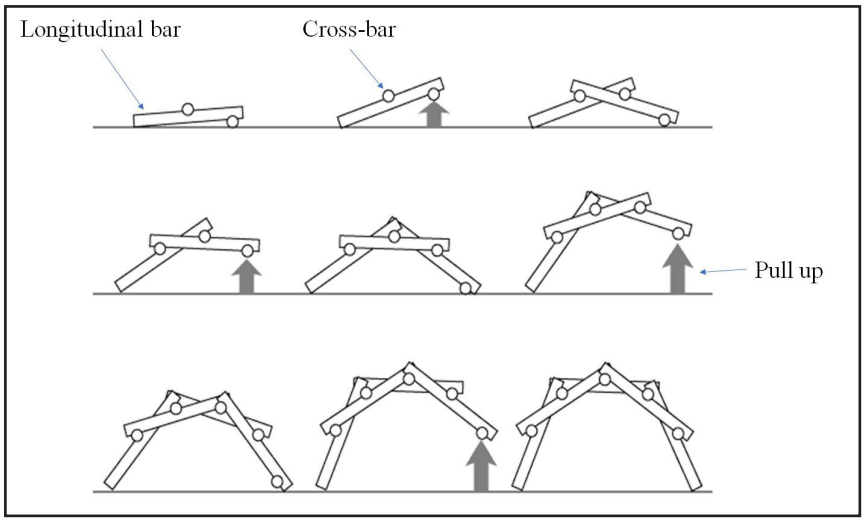

Source: Na Engenharia! (2022)

The connections between the bars influence the way loads are transmitted among them. Given the simplicity of the bridge and its self-supporting characteristic, the internal connections can be articulated without compromising the stability of the structure. One way to construct it is to only restrict the horizontal displacement of the inclined longitudinal bars, locking the lower side.

In Figure 3(a), Support 1 is a double support as it prevents movement both perpendicular and parallel to the bar axis. Support 2 is a single support, only preventing

movement perpendicular to the axis. Upon observing the bridge's structure (Figure 3(b)), it is noted that the cross-bars play the role of supports. Furthermore, each longitudinal bar has a different angle (θ) defined in the Cartesian plane.

Figure 3 – Double-supported bar with inclination θ with respect to the horizontal (a); cross-bars as supports (b)

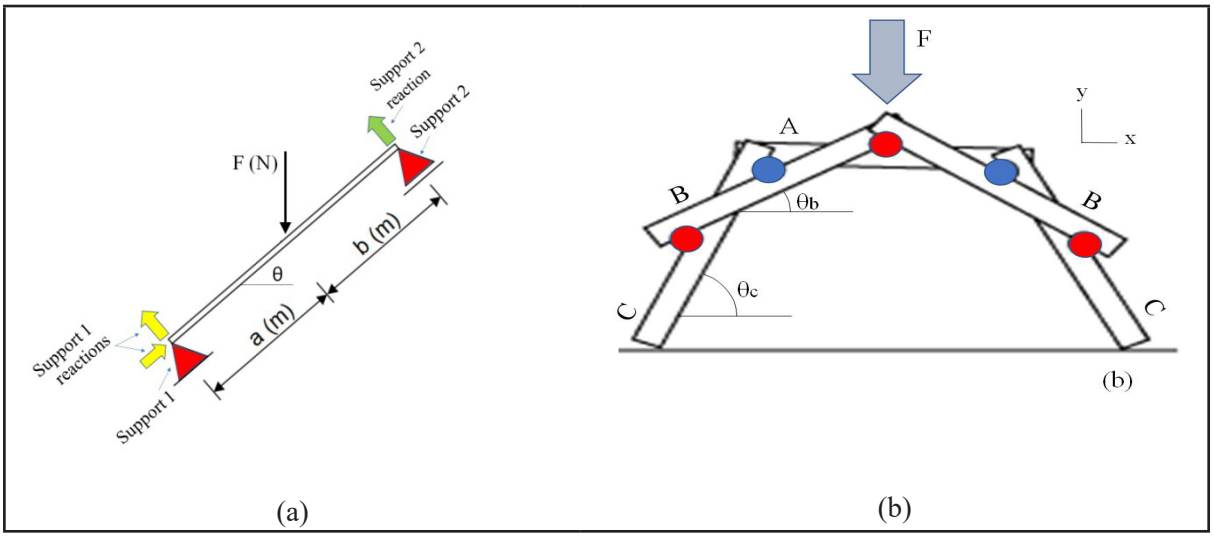

Source: authors (2024)

In this study, the aim was to derive the support reactions equations for the bars to perform various designs of the self-supporting bridge, using wood as the material, and assess the possibilities for a theoretical loading scenario.

2 METODOLOGY

2.1 Bridge geometry

The central bars, labeled as A-bar (Figure 3(b)), are horizontally positioned, therefore having their angle (θ_a - not shown in the figure) equal to zero with respect to the horizontal x-axis. The B-bar will have an angle 'θ_b,' and the C-bar will have an angle 'θ_c,' all with respect to the x-axis. The bridge may have additional longitudinal bars beyond bars A, B, and C, as seen in Da Vinci's drawing (Figure 1). Naturally, a bridge

with multiple longitudinal bars complicates its assembly. For calculation, simplification, and practicality in real-world assembly, we will develop equations for a bridge with only bars A, B, and C. The angles of the longitudinal bars will be calculated based on the measurements of the longitudinal bars and cross-bars.

Another important aspect is calculating the span of the bridge and its maximum height reached. To perform these calculations, the angle and length of each longitudinal bar (L) are employed. In this article, the same length will be adopted for all longitudinal bars. This simplification aids in the calculation and execution of the bridge.

2.2 Acting forces

Two loadings were considered in the structure: a concentrated force (F) at the center of the bridge, as it represents the worst-case of external static loading scenario for the bridge, and the self-weight of the bridge bars. The concentrated force depends on the load that will traverse the bridge, which could be the equivalent weight of a vehicle, a person, etc. The self-weight of the bars depends on the wood used, as the specific mass of distinct woods influences the linear density weight (q) differently. By multiplying the linear weight of the bar (q) by its length (L), we obtain the total weight of the longitudinal bar (P). The cross-bars will also have their weight distributed on the bridge. In this case, the self-weight of each cross-bar (T) becomes a concentrated load at the center of a longitudinal bar.

As the loading is dissipated towards the bridge's edges, the more inclined bars end up demanding more from the double support (Figure 3(a), Support 1). The most central bars (A-bar - Figure 3(b)) primarily exhibit the internal force called bending, and the bars at the edges (C-bar - Figure 3(b)) exhibit the compression force, along with a less pronounced bending (ABAD, 2021). This fact will be verified explicitly in the results in 3.3.2.

2.3 Reactions of the Longitudinal Bars

Each longitudinal bar of the bridge has its vertical (R_v) and horizontal (R_h) support reactions. Given the symmetry of the loading and supports, R_v has the same magnitude on both sides of the bars; thus, they were not differentiated in the calculation.

Figure 4 depicts the loading on the A-bar. The 'F' load is an external load positioned at the center of the bridge, the 'T' load is the weight of the cross-bar in the center, the distributed load 'q' is the linear density weight of the A-bar, and the 'R_{vb}' loads are support reactions from the B-bar (one on each side) that unload onto the central cross-bar with an angle $-\theta_b$ and $+\theta_b$. The two support reactions from the B-bars form a vertical vector (R_{vb}').

Figure 4 – Loading on the A-bar

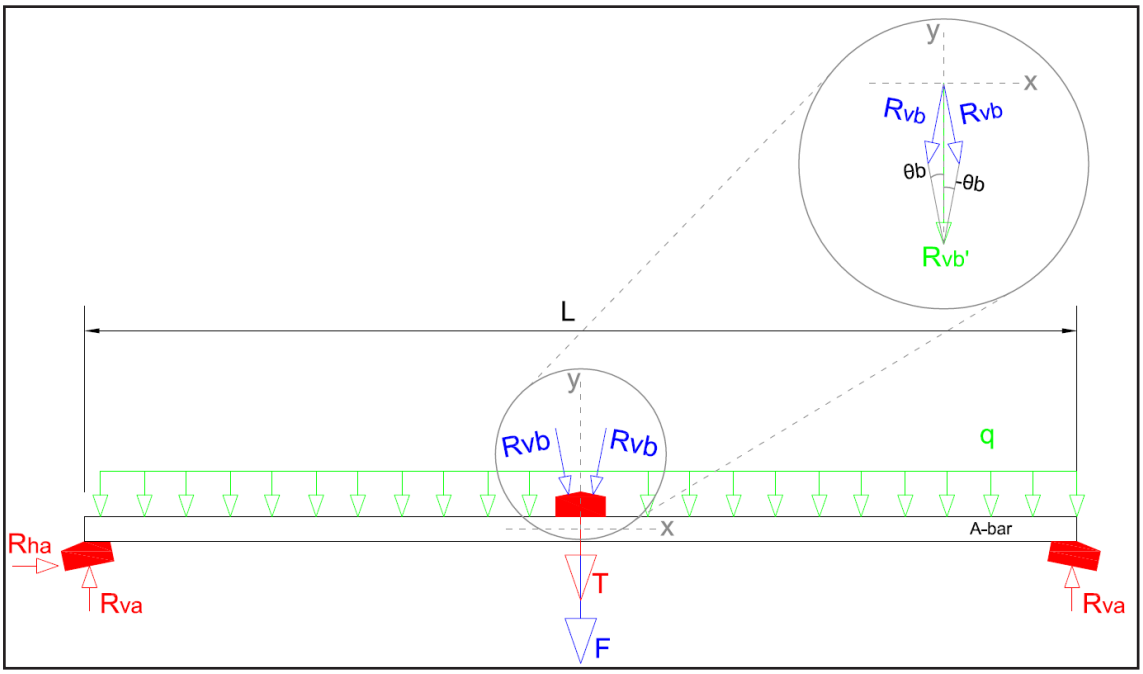

Source: authors (2024)

Through the equations of statics (Hibbeler, 2009), we have that the support reactions of the A-bar are:

$$R_{ha} = 0 \quad (1)$$

$$R_{va} = \frac{P+T}{2} + \frac{F}{2} + R_{vb}\cos\theta_b \tag{2}$$

The B-bar (Figure 5) experiences the action of a central cross-bar (T), its own weight represented by Equation 3, and the support reactions from bars A and C on the central cross-bar, oriented at angles $-\theta_b$ and $+\theta_b$, respectively, with respect to the axis perpendicular to bar B.

$$P = q\,L \tag{3}$$

Figure 5 – Loading on the B-bar

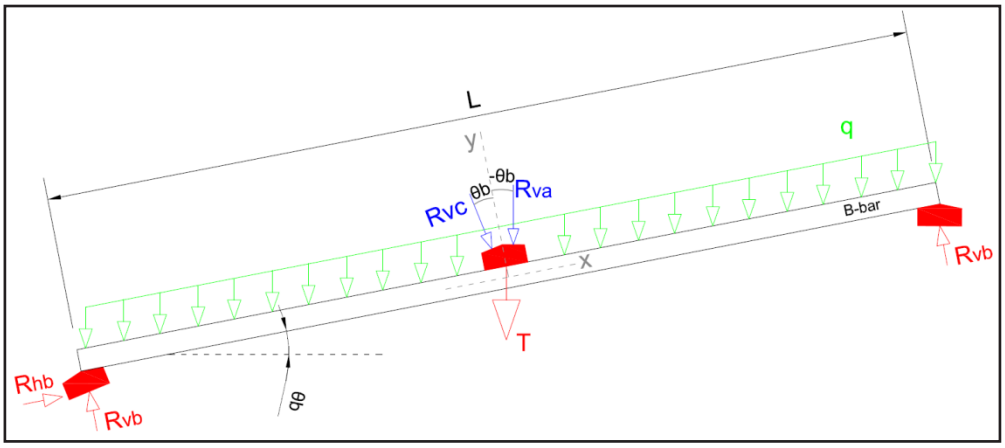

Source: authors (2024)

Therefore, the reactions are given by:

$$R_{hb} = (P+T)\,sen\theta_b + R_{va}\,sen\theta_b - R_{vc}\,sen\theta_b \tag{4}$$

$$R_{vb} = \frac{P+T}{2}\cos\theta_b + R_{va}\frac{\cos\theta_b}{2} + R_{vc}\frac{\cos\theta_b}{2} \tag{5}$$

As support reactions of the B-bar (Equations 4 and 5) are, therefore, dependent on the support reactions of bars A and C. It is noteworthy that the reactions of the B-bar, called vertical and horizontal (R_{vb} and R_{hb}), are not oriented according to the reactions of the A-bar but rather along the axis of the B-bar. In other words, the

vertical reaction is perpendicular to the axis of B-bar, and the horizontal reaction is parallel to the axis of B-bar.

Considering that we have only bars A, B, and C in the bridge structure, the C-bar, in addition to being supported by the B-bar (Figure 6), is also supported by the ground.

Figure 6 – Loading on the C-bar

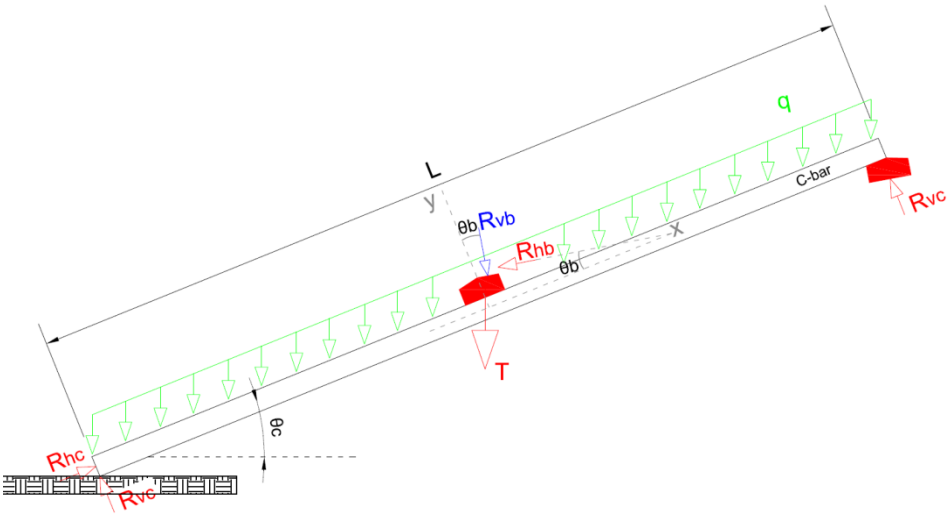

Source: authors (2024)

Differently from the other bars, only one support reaction unloads onto the central cross-bar from C: the vertical reaction from the B-bar (R_{vb}), with an angle of θ_b. We have the other loadings of this bar – its own weight (P) and the weight of the cross-bar (T). The support reactions of C will be:

$$R_{hc} = (P+T)sen\theta_c + R_{vb}\, sen\theta_b + R_{hb}\cos\theta_b \tag{6}$$

$$R_{vc} = \frac{P+T}{2}\cos\theta_c + R_{vb}\frac{\cos\theta_b}{2} - R_{hb}\, sen\theta_b \tag{7}$$

The support reactions of the C-bar (Equations 6 and 7) depend on the support reactions of the B-bar. Similar to the case the B-bar, the support reactions of the C-bar are oriented along the axis of the bar itself.

With these equations, the support reactions of the longitudinal bars form a system of coupled equations. Algebraic manipulations were performed to obtain the support reactions depending on the following constants: the weight of the longitudinal bar (P), the weight of the cross-bar (T), the angles of the bars (θ), and the concentrated force applied at the center of the bridge (F).

2.4 Design of the wooden bridge

Based on the support reactions of each bar, efforts were made to determine the internal forces (normal force, shear force, and bending moment) (HIBBELER, 2009) along each bar to then carry out the sizing of the bars, adopting the largest dimension obtained from the calculations of normal stress, simple straight bending and longitudinal shear.

The technical standard NBR 7190:2022 was used for the design of the longitudinal bars. Modification coefficients for calculating wood strength were K_{mod1} of 0.6 (permanent load) and K_{mod2} of 0.8 (moisture class 3, with ambient humidity between 75% and 85%). Reduction coefficients for the ultimate limit state were 1.4 for normal stresses and 1.8 for shear stresses.

The chosen wood for design is hardwood, category D60 from table 3 of standard NBR 7190-1:2022. The characteristic tensile strength parallel to the fibers is 36 MPa, the characteristic compressive strength is 32 MPa, the shear strength is 4.5 MPa, and the density is 700 kg/m^3.

A rectangular cross-sectional shape was adopted for the longitudinal bars, and a trapezoidal cross-sectional shape for the cross-bars (Figure 7), ensuring maximum contact between the cross-bar and longitudinal bars.

Figure 7 – Cross-section of the longitudinal bars and cross-bars

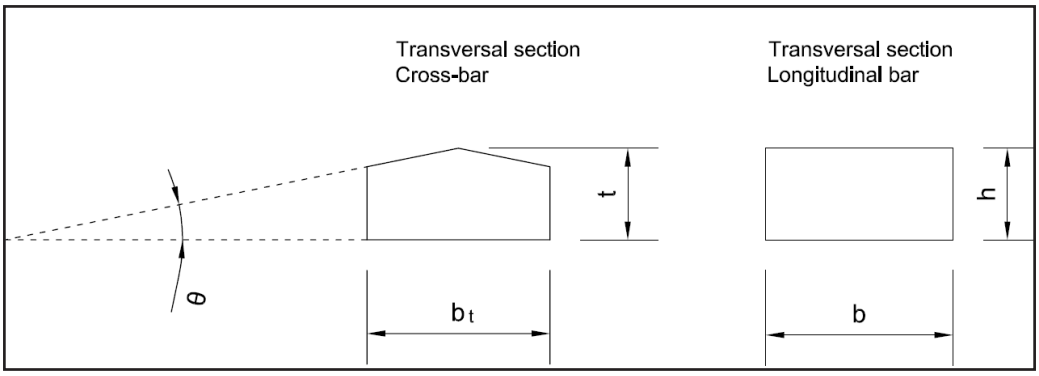

Source: authors (2024)

The design of the cross-bars was not the focus of this research. Thus, a fixed length of 2 meters was defined for the cross-bars, and the cross-sectional dimensions were set to match those of the longitudinal bars after their design. Therefore, the dimension 't' was made equal to the dimension 'h' (obtained during design), and the dimension 'b_t' equal to the dimension 'b'.

Four longitudinal bars were considered in each section, meaning the bar labeled A consists of 4 bars arranged side by side, the B-bar consists of 4 bars to the left of A and 4 bars to the right of A, as can be seen in Figure 8.

Figure 8 – Perspective of the self-supporting bridge under study

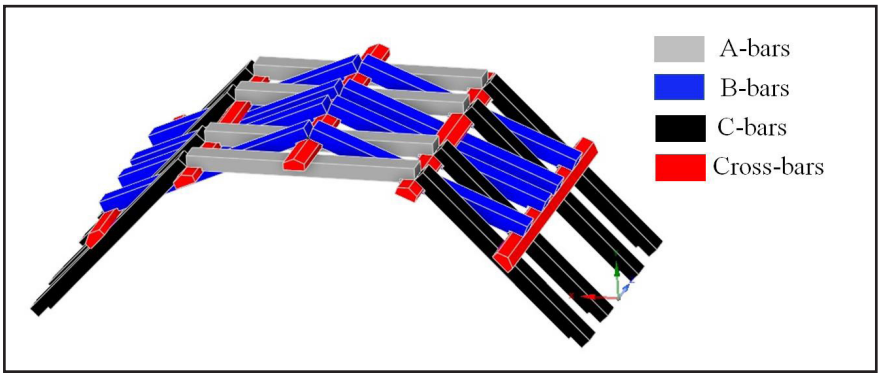

Source: authors (2024)

For simulations of different bridge execution possibilities, according to design, a concentrated force at the center of the A-bar was established, fixed at 20,000 N (approximately 2 tons, equivalent to a heavy-duty passenger car), and bridge spans ranging from 4 to 7 meters. The self-weight of the wooden bars was obtained by calculating the volume (cross-sectional area times length) multiplied by the wood density (700 kg/m^3).

3 RESULTS AND DISCUSSIONS

3.1 Bridge geometry

To determine the angle of the bars, a right-angled triangle was constructed using the measurements of the longitudinal bars and cross-bars (Figure 9).

Figure 9 – Angle of the B-bar in relation to A-bar

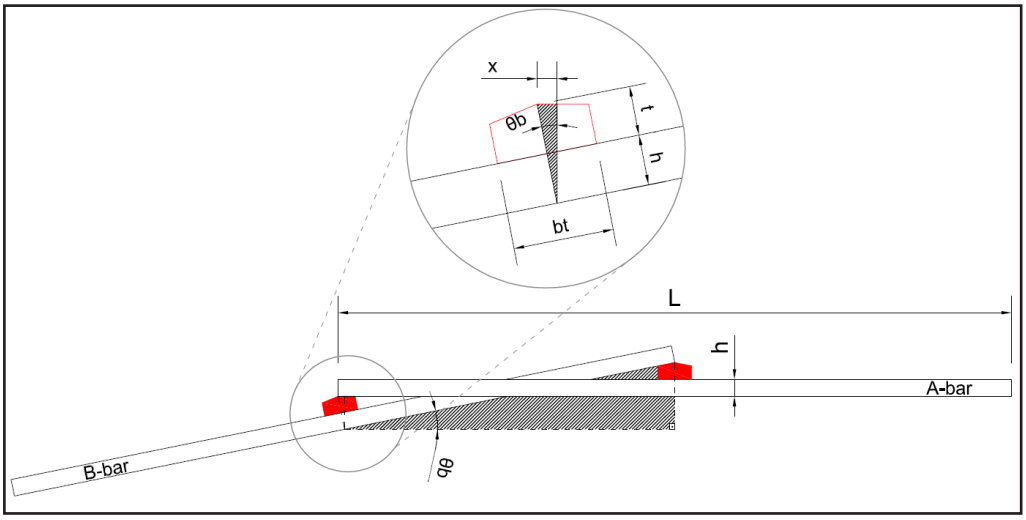

Source: authors (2024)

From the larger right-angled triangle, we have:

$$\cos \theta_b = \frac{\frac{L}{2} - x}{\frac{L}{2}} \tag{8}$$

As the measure x depends on the same angle θ of the B-bar, according to the smaller right-angled triangle, we have:

$$x = (t + h)\cos\theta_b \tag{9}$$

Substituting Equation 9 into Equation 8, we obtain the angle of the B-bar (Equation 10):

$$\theta_b = 2\left[arctg\left(2\frac{t+h}{L}\right)\right] \tag{10}$$

By performing an analogous calculation, we can determine the angles of more inclined bars, such as C, D, and E. As depicted in Table 1, the corresponding angles are multiples of the angle θ_b.

Table 1 – Angles of the longitudinal bars

Bar	Angle
A	$\theta_a = 0$
B	θ_b
C	$\theta_c = 2\theta_b$
D	$\theta_d = 3\theta_b$
E	$\theta_e = 4\theta_b$

Source: authors (2024)

For the calculation of the span (Figure 10), a bridge was considered with longitudinal bars A, B, and C, all of equal length, with their respective angles θ (Table 1) calculated earlier.

Figure 10 – Measurements for the calculation of the total span and height H of the bridge

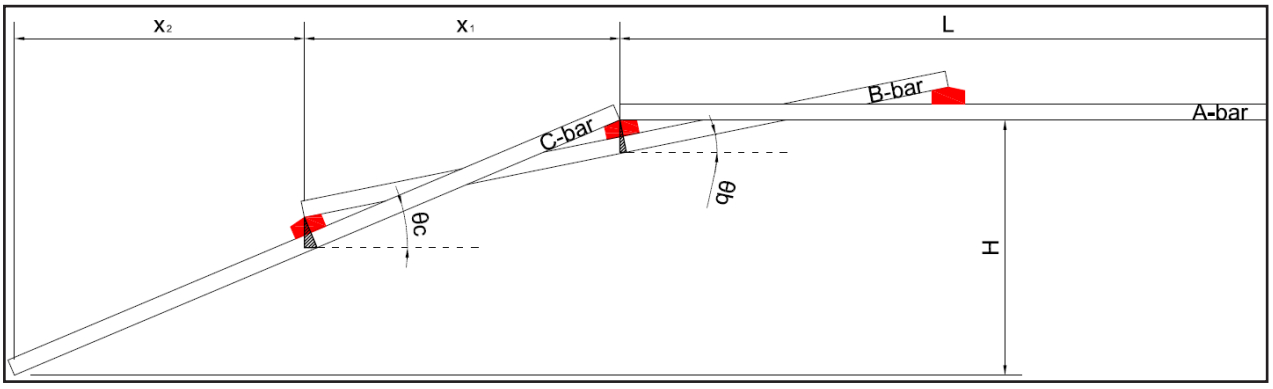

Source: authors (2024)

The total span (L_t) of the bridge will be:

$$L_t = L + 2(x_1 + x_2) \tag{11}$$

Since the measures x_1 and x_2 are dependent on angles θ_b and θ_c, respectively, we have:

$$L_t = L\cos\theta_a + L\cos\theta_b + L\cos\theta_c - 2(t+h)(\operatorname{sen}\theta_b + \operatorname{sen}\theta_c) \tag{12}$$

The height (H) of the bridge depends on the chosen initial and final points, and it will be given by:

$$H = \frac{L}{2}(\operatorname{sen}\theta_b + \operatorname{sen}\theta_c) + (t+h)(\cos\theta_b + \cos\theta_c) \tag{13}$$

3.2 Support Reactions

Table 2 presents the vertical and horizontal reactions of bars A, B, and C. Trigonometric operations were used to express them solely in terms of the angle of the B-bar (θ_b).

Table 2 – Results of the support reactions of bars A, B, and C

Bar	Reaction	Intensity
A	R_{ha}	0
	R_{va}	$\frac{12\cos^2\theta_b - 3}{-8\cos^2\theta_b + 10}(P+T) + \frac{3}{-8\cos^2\theta_b + 10}F$
B	R_{hb}	$\frac{4\operatorname{sen}\theta_b\cos^4\theta_b - 9\operatorname{sen}\theta_b\cos^2\theta_b + 8\operatorname{sen}\theta_b}{-4\cos^4\theta_b + 5\cos^2\theta_b}(P+T) + \frac{-\operatorname{sen}\theta_b\cos^2\theta_b + 2\operatorname{sen}\theta_b}{-4\cos^4\theta_b + 5\cos^2\theta_b}F$
	R_{vb}	$\frac{8\cos^2\theta_b - 4}{-4\cos^3\theta_b + 5\cos^2\theta_b}(P+T) + \frac{2\cos^2\theta_b - 1}{-4\cos^3\theta_b + 5\cos^2\theta_b}F$
C	R_{hc}	$\frac{-4\operatorname{sen}\theta_b\cos^4\theta_b + 9\operatorname{sen}\theta_b\cos^2\theta_b + 4\operatorname{sen}\theta_b}{-4\cos^5\theta_b + 5\cos\theta_b}(P+T) + \frac{\operatorname{sen}\theta_b\cos^2\theta_b + \operatorname{sen}\theta_b}{-4\cos^3\theta_b + 5\cos\theta_b}F$
	R_{vc}	$\frac{-4\cos^4\theta_b + 25\cos^2\theta_b - 16}{-8\cos^4\theta_b + 10\cos^2\theta_b}(P+T) + \frac{5\cos^2\theta_b - 4}{-8\cos^4\theta_b + 10\cos^2\theta_b}F$

Source: authors (2024)

One can observe that the vertical and horizontal reactions have a common denominator of () and the weight loads (from the longitudinal bar, P, and cross-bar, T) and the applied force (F) have distinct multipliers. Additionally, there are no significant similarities between the equations to establish a pattern for creating a general formula.

3.3 Simulation of data

3.3.1 Design and Geometric Modifications of Bridges

In the design of the longitudinal bars, two fundamental design variables are crucial: the span intended to be achieved and the force to be considered on the bridge. Table 3 presents the result of the design for different construction possibilities. The goal was to find a bridge with a maximum inclination of 45º for ease of crossing and a maximum width of the bars of 30 cm to facilitate material acquisition and limit weight. Options exceeding these limitations were marked with an asterisk.

Table 3 – Results of the bridge design with spans of 4, 5, 6, and 7 m

Bridge		**Longitudinal bars**						**Cross-bars**	
Span (m)	**Height (m)**	**L (m)**	**θ_b**	**θ_c**	**Height (h) (cm)**	**Width (b) (cm)**	**1 bar weight (N)**	**Height (t) (cm)**	**Width (bt) (cm)**
4,00	1,14	1,63	21,95	43,90	8	42*	383,4	8	42*
	1,37	1,77	25,47	50,94*	10	24	297,4	10	24
	1,59	1,90	28,36	56,72*	12	15	239,4	12	15
5,00	1,43	2,05	22,08	44,16	10	34*	487,9	10	34*
	1,66	2,18	24,83	49,66*	12	21	384,6	12	21
	1,88	2,31	27,25	54,50*	14	15	339,6	14	15
6,00	1,72	2,47	22,00	44,00	12	29	601,7	12	29
	1,95	2,59	24,40	48,80*	14	20	507,6	14	20
	2,17	2,72	26,48	52,96*	16	15	456,9	16	15
7,00	1,75	2,75	19,80	39,60	12	40*	924,0	12	40*
	2,00	2,87	22,08	44,16	14	27	759,4	14	27
	2,24	3,00	24,08	48,16*	16	19	638,4	16	19

* Values that exceed the stipulated limits

Source: authors (2024)

To reduce the inclination of the bridge (θ_c), it was necessary to reduce the height of the bars, demanding an increase in their width. For bridges with a span of 4m, the only simulation that resulted in an angle of the C-bar below 45° was with a bar height of 8 cm. This alternative has a base measurement almost 3 times higher than the option with a height of 12 cm, and each longitudinal bar's weight is 60% higher, causing an increase in cost. The three bridge options for the 4-meter span are shown in Figure 11.

Figure 11 – Possibilities for a bridge with a 4-meter span

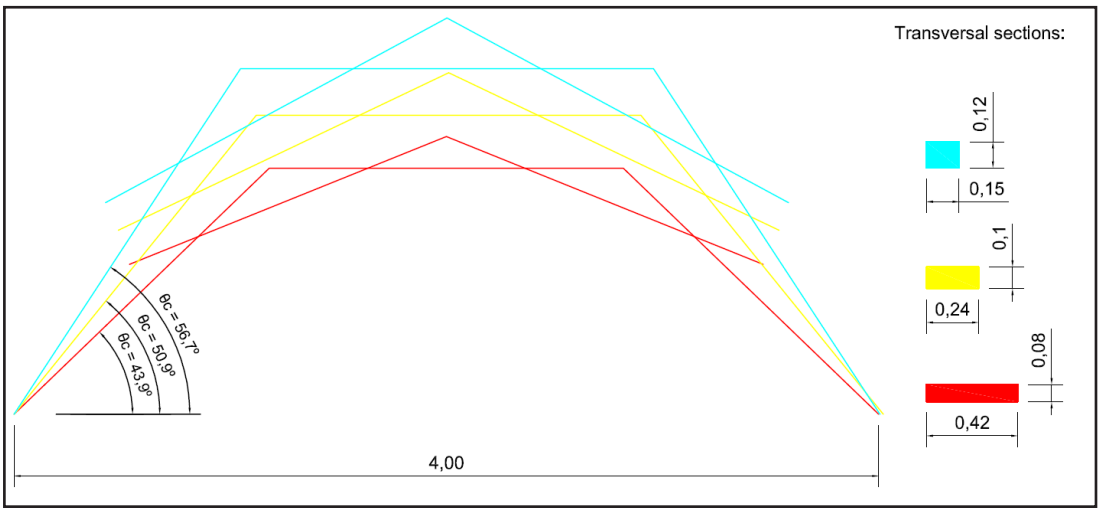

Source: authors (2024)

Similarly, bars with heights of 12 cm and 14 cm generated an angle θ_c above 45° in bridges with a span of 5 m. Alternatively, bars with a height of 10 cm reduced the angle and increased the width of the bars.

For the 6m span bridge, the simulation with bars of 12x29 cm cross-section generated a suitable bridge with angles below 45°. However, for the 7-meter span bridge, the best option to maintain the angle of the C-bar below 45° and an appropriate transversal section area was 14x27 cm.

It is also possible to observe that, keeping the height of the longitudinal bars constant, an increase of approximately 28 cm in the length of the bars was necessary

to increase the span of the bridge by 1 m. For example, with a height of 12 cm, bars of 1.90 m were needed to achieve a 4 m bridge, bars of 2.18 m for a 5 m bridge, bars of 2.47 m for a 6m bridge, and bars of 2.75 m for a 7 m bridge. As this increase in length occurred, the angle of the C bars decreased.

3.3.2 Force transmission

To analyze the intensity of the support reactions, only the option of a 6-meter span bridge was considered, with a transversal section area of 12x29 cm for bars and cross-bars, and a length of 2.47 m for the bars. The weight (P) of each longitudinal bar was 601.7 N, and the weight of each cross-bar was 487.2 N.

Table 4 presents the vertical (R_v) and horizontal (R_h) support reactions of bars A, B, and C, specifying the intensity originating from the self-weight (P and T) and the intensity caused by the force (F), which again is considered to be of 20,000 N.

Table 4 – Vertical and horizontal support reactions of bars A, B, and C

Bar	Angle	Vertical reaction (N)			Horizontal reaction (N)		
		Self-weight	Force/load	Total	Self-weight	Force/load	Total
A	0º	6782.1	19217.7	25999.8	0.0	0.0	0.0
B	22.0º	5753.9	8567.6	14321.5	2599.6	6364.0	8963.5
C	44.0º	2735.0	2225.4	4960.5	6575.3	9624.0	16199.2

Source: authors (2024)

It is observed that the largest support reaction is vertical in the central bars, referred to as A-bar. In the intermediate B-bars, which in this situation have an inclination of 22º, their vertical reaction is greater than the horizontal reaction for this configuration. In the more inclined C-bars, the vertical reaction is less than the horizontal reaction. In other words, the loads dissipate towards the bases, intensifying the internal force in the direction of the bar axis (horizontal force) and gradually reducing the force in the direction perpendicular to the axis (vertical force).

The externally applied force (F) generated a greater intensity of internal force in bars A, B, and C when compared to the self-weight of the structure. However, this is a particularity of this simulated configuration, with a force of 20,000 N.

3.3.3 Effects on total weight and bridge efficiency

Each previous design results in a total weight of the bridge (wood weight only). Table 5 presents the results of different options for the four span measurements, including some intermediate possibilities not previously shown.

Table 5 – Geometric data and weight of bridges with spans of 4, 5, 6, and 7 m

Geometry				Weight		
Span (m)	**Height (m)**	**Height-to-span ratio**	**Lenght of each bar (m)**	**Bridge (N)**	**Force/ load (N)**	**Load-to-weight ratio**
4.00	1.14**	0.28	1.63	10463.2	20,000	1.91
	1.26*	0.31	1.71	8723.8		2.29
	1.37*	0.34	1.77	7965.0		2.51
	1.48*	0.37	1.84	7526.4		2.66
	1.59*	0.40	1.90	6315.8		3.17
5.00	1.43**	0.29	2.05	12675.5	20,000	1.58
	1.55*	0.31	2.12	11376.4		1.76
	1.66*	0.33	2.18	9873.8		2.03
	1.77*	0.35	2.25	9408.0		2.13
	1.88*	0.38	2.31	8627.3		2.32
6.00	1.72	0.29	2.47	15110.6	20,000	1.32
	1.83*	0.30	2.53	13821.2		1.45
	1.95*	0.33	2.59	12649.2		1.58
	2.06*	0.34	2.66	11780.8		1.70
	2.17*	0.36	2.72	10819.2		1.85
7.00	1.75**	0.25	2.75	22807.2	20,000	0.88
	1.88**	0.27	2.81	20131.2		0.99
	2.00	0.29	2.87	18623.8		1.07
	2.12*	0.30	2.94	17351.0		1.15
	2.24*	0.32	3.00	15555.7		1.29

* Bridges with an angle of bar C greater than 45º

** Bridges with bars wider than 30 cm

Source: authors (2024)

The height-to-span ratio of the bridge varied from 0.25 to 0.40. In options for the same span, the weight of the bridge decreased as the height of the bridge increased, despite the increase in the length of the longitudinal bars. This is due to the considerable reduction in the transversal section area obtained in the design process. With the increase in the height of the bridge, the angle of the C-bar also increased, reaching approximately 45º in some cases.

If we consider that the efficiency of the bridge is relative to how many times it can support its own weight, the last column thus becomes an indirect parameter of efficiency. Given that the load was fixed at 20,000 N, bridges with lower weight, for each span, had better efficiency. In this case, bridges with greater heights had better results.

As the span increased, the efficiency of the bridges decreased, ranging from load-to-weight ratios of 2 to 3 for 4 m span bridges to approximately 1 for 7 m span bridges. For example, for a span of 4 m, the bridge with the greatest height is capable of supporting a load 3.17 times its own weight. On the other hand, 7 m span bridges are able to support a load approximately equal to their own weight, as they had load-to-weight ratios ranging from 0.88 to 1.29.

Under the defined boundary conditions, the best option was the bridge for a 6 m span with a height of 1.72 m. This option met the criteria for angle and width of bars and had the best efficiency in the load-to-weight ratio.

Figure 12 presents the angle of C-bar (θ_c) according to the height-to-span ratio of the bridges. It was observed that bridges with a height-to-span ratio of 0.3 or more had an angle of C-bar greater than 45º, regardless of the span to be overcome. Angles greater than 45º make the bridge quite steep for crossing.

Figure 12 – Height-to-span ratio versus angle of the C-bar for bridges of 4, 5, 6, and 7 m

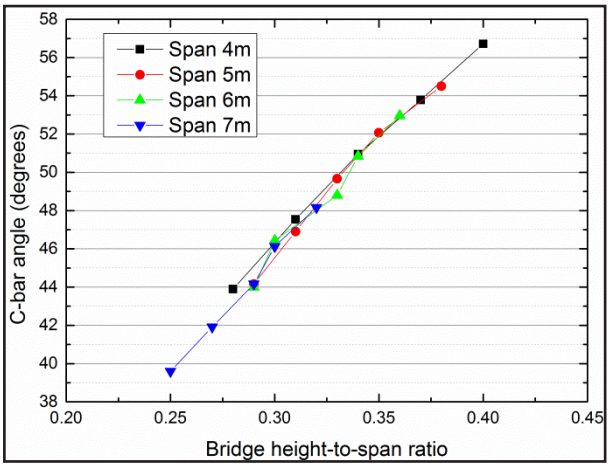

Source: authors (2024)

Figure 13 presents the height-to-span and load-to-weight ratios in graphical form.

Figure 13 – Height-to-span ratio versus load-to-weight ratio for bridges of 4, 5, 6, and 7 m

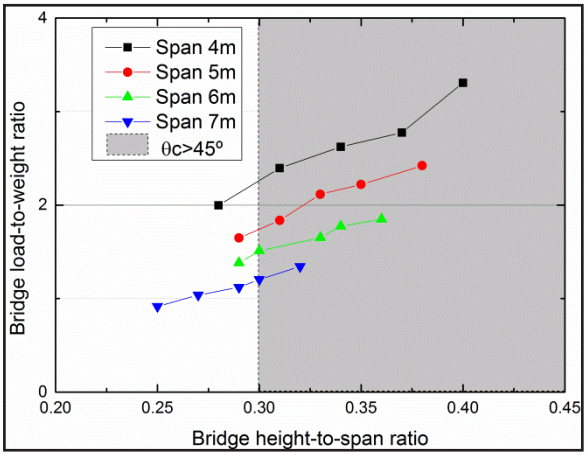

Source: authors (2024)

For each bridge span, there is an efficiency limit (load-to-weight ratio) before reaching the region with an angle greater than 45°. The smaller the span, the greater the efficiency of the bridge. Bridges with a span of 7 meters showed a load-to-weight ratio close to 1, as the weight of the designed bridge approached the simulated load of 20,000 N. It is expected that, for the same loading, longer bridges will have even lower

efficiency, with their own weight exceeding 20,000 N. The best alternative in this case would be to design a bridge with a height-to-span ratio of 0.30 to avoid exceeding the 45º inclination and achieve the best load-to-weight ratio.

4 CONCLUSIONS

It was possible to obtain geometric formulations for the self-supporting bridge designed by Leonardo Da Vinci. By adopting a bridge composition with bars labeled A, B, and C, proportional inclinations were obtained, where the central bar's inclination is zero, and the edge bar (C) has an inclination twice that of the intermediate bar (B). Subsequently, it was possible to determine the support reactions of the longitudinal bars, necessary for calculating internal forces. The internal forces, in turn, are essential for the dimensioning of the bars.

Through simulations, it was found that there are numerous construction possibilities for a given span. The variation in the length and height of bars and crossbars guides the geometric characteristics of the bridge's span and maximum height. A very steep inclination provides a lighter and more efficient bridge, but it makes crossing in a practical situation challenging.

The calculation of support reactions shows that the central longitudinal bars (A) only have a vertical reaction (perpendicular to the axis), the intermediate bars (B) have both vertical and horizontal reactions, and the edge bars (C) have a greater horizontal support reaction (parallel to the bar axis).

For the dimensioning of the bars, simulations were performed for spans of 4 meters, 5 meters, 6 meters, and 7 meters. It was observed that to avoid a steep inclination of the edge bars (C), it is necessary to increase the width of the cross-sectional area of the longitudinal bars. This results in greater weight and lower efficiency of the bridge. Considering a limit of 45º inclination for the edge bars of the bridge, it is necessary to respect the height/span ratio of 0.30, thus obtaining the best option for efficiency and usability.

Furthermore, noticing the somewhat steep entrance angles , it is possible to design an adaptation at the entrance (and exit) of the bridge to facilitate the access of bridges with inclinations of 45º or even steeper angles, through ramps with inclinations lower than the C-bar, supported by the outermost cross-bars, with the same angle , for example, which would be half the entrance angle as can be seen in Table 3. However, the ramp would introduce an additional load on the structure that would need to be carefully studied to prevent potential ruptures.

REFERENCES

Abad, Carla Torres. (2021). Eficiencia del puente autoportante de Leonardo. *Técnica Industrial*, 328, 30-37.

ABNT (Associação Brasileira de Normas Técnicas). (2022). *NBR 7190 – Projeto de estruturas de madeira. Parte 1: Critérios de dimensionamento.* Rio de Janeiro: ABNT.

Engenho E Arte. (2020). *A ponte de emergência para a outra margem de Leonardo Da Vinci.* Retrieved from:https://www.engenhoearte.info/post/a-ponte-de-emerg%C3%AAncia-para-a-outra-margem-de-leonardo-da-vinci.

Hibbeler, R. C. (2009). *Resistencia dos materiais.* 7.ed. Sao Paulo: Pearson Prentice Hall.

Hipátia Engenharia.(2022). *Ponte de Leonardo da Vinci (Self-Supporting Bridge).* Retrieved from: http://www.hipatiaengenharia.com.br/2022/08/ponte-de-leonardo-da-vinci.html, 2022.

Lima, G. F. A., Perassi, R., & Triska, R. (2017). *O design de Leonardo da Vinci do ponto de vista filosófico e científico.* Colóquio Internacional de Design.

Morumbi Sul. (2021). *Construindo pontes com Da Vinci.* Retrieved from: https://morumbisul.com.br/construindo-pontes-com-da-vinci/.

Na Engenharia!. (2022). *A Incrível Ponte Projetada por Leonardo Da Vinci.* Retrieved from: http://naengenhariablog.blogspot.com/2017/01/a-incrivel-ponte-projetada-por-leonardo.html.

Authorship contributions

1 – Lucas Alves Lamberti

Doutor em Engenharia Civil, Professor da Universidade Federal de Santa Maria.
https://orcid.org/0000-0002-5004-5288 - lucas.lamberti@ufsm.br
Contribuição: Data curation, investigation, writing

2 – Rafael Domingues Della Pace

Doutor em Física, Professor da Universidade Federal de Santa Maria
https://orcid.org/0000-0003-4406-9512 - rafael.pace@ufsm.br
Contribuição: writing – review and editing

3 – Lucas Tavares Cardoso

Doutor em Física, Professor da Universidade Federal de Santa Maria
https://orcid.org/0000-0002-7878-3776 - lucas.cardoso@ufsm.br
Contribuição: Formal analysis, supervision

4 – Carla Fernanda Perius

Doutora em Engenharia Civil, Técnica Administrativa na Universidade Federal de Santa Maria
https://orcid.org/0000-0001-6336-6286 - carla.perius@ufsm.br
Contribuição: Conceptualization, supervision

5 – Fábio Beck

Doutor em Física, Professor da Universidade Federal de Santa Maria
https://orcid.org/0000-0003-0502-6827 - fabiobeckster@gmail.com
Contribuição: writing – review and editing

6 – Diogo Pauletti

Doutor em Física, Professor da Universidade Federal de Santa Maria
https://orcid.org/0009-0000-5035-4374 - diogo.pauletti@ufsm.br
Contribuição: Formal analysis, supervision

How to quote this article

Lamberti, L. A., Della Pace, R. D., Tavares, L. C., Perius, C. F., Beck, F. & Pauletti, D. (2024). Structural analysis and design of a self-supporting wooden bridge designed by Leonardo Da Vinci. *Ciência e Natura*., Santa Maria, 46, e86798 https:// doi.org/10.5902/2179460X86798